A noncatalytic function of the ligation complex during nonhomologous end joining

Jessica Cottarel,[1,2] Philippe Frit,[1,2] Oriane Bombarde,[1,2] Bernard Salles,[1,2] Aurélie Négrel,[5,6,7,8] Stéphanie Bernard,[5,6,7,8] Penny A. Jeggo,[3] Michael R. Lieber,[4] Mauro Modesti,[5,6,7,8] and Patrick Calsou[1,2]

[1]Centre National de la Recherche Scientifique, Institut de Pharmacologie et de Biologie Structurale, Toulouse F-31077, Cedex 4, France
[2]Université de Toulouse-Université Paul Sabatier, Institut de Pharmacologie et de Biologie Structurale, Toulouse F-31077, Cedex 4, France
[3]Genome Damage and Stability Centre, University of Sussex, East Sussex BN1 9RQ, England, UK
[4]Norris Comprehensive Cancer Center, University of Southern California Keck School of Medicine, Los Angeles, CA 90089
[5]Centre de Recherche en Cancérologie de Marseille, Centre National de la Recherche Scientifique, Unité Mixte de Recherche 7258, Marseille F-13009, France
[6]Institut National de la Santé et de la Recherche Médicale, U1068, Marseille F-13009, France
[7]Institut Paoli-Calmettes, Marseille F-13009, France
[8]Aix-Marseille Université, Marseille F-13284, France

Nonhomologous end joining is the primary deoxyribonucleic acid (DNA) double-strand break repair pathway in multicellular eukaryotes. To initiate repair, Ku binds DNA ends and recruits the DNA-dependent protein kinase (DNA-PK) catalytic subunit (DNA-PKcs) forming the holoenzyme. Early end synapsis is associated with kinase autophosphorylation. The XRCC4 (X4)–DNA Ligase IV (LIG4) complex (X4LIG4) executes the final ligation promoted by Cernunnos (Cer)–X4-like factor (XLF). In this paper, using a cell-free system that recapitulates end synapsis and DNA-PKcs autophosphorylation, we found a defect in both activities in human cell extracts lacking LIG4. LIG4 also stimulated the DNA-PKcs autophosphorylation in a reconstitution assay with purified components. We additionally uncovered a kinase autophosphorylation defect in LIG4-defective cells that was corrected by ectopic expression of catalytically dead LIG4. Finally, our data support a contribution of Cer-XLF to this unexpected early role of the ligation complex in end joining. We propose that productive end joining occurs by early formation of a supramolecular entity containing both DNA-PK and X4LIG4–Cer-XLF complexes on DNA ends.

Introduction

Double-strand breaks (DSBs) are lesions that, if improperly repaired, can cause cell death or cancer after genomic rearrangement (O'Driscoll and Jeggo, 2006). In mammalian cells, DSBs initiate a global cellular response including checkpoint signaling and repair (Polo and Jackson, 2011). Nonhomologous end joining (NHEJ), the major pathway in mammalian cells, operates throughout the cell cycle. NHEJ is intrinsically versatile, handling a wide variety of DNA end configurations, and ligates two DNA ends after limited end processing (Wyman and Kanaar, 2006; Hartlerode and Scully, 2009; Pardo et al., 2009; Lieber, 2010).

NHEJ proceeds via at least three steps: (1) break recognition/repair initiation, (2) processing of the damaged DNA ends by nucleases and polymerases, and (3) ligation to complete DSB repair (Weterings and Chen, 2008; Lieber, 2010). The initiating event is the binding of the Ku70/Ku80 heterodimer to DNA ends (Downs and Jackson, 2004). Most of the known NHEJ components interact with Ku (Lieber, 2010). Live-cell imaging experiments after laser microirradiation indicate that core NHEJ components are independently recruited to Ku-bound DSBs (Yano and Chen, 2008), including the DNA-dependent protein kinase (DNA-PK) catalytic subunit (DNA-PKcs), Cernunnos (Cer)–XRCC4 (X4)-like factor (XLF), and the preassembled X4–DNA Ligase IV (LIG4) complex (X4LIG4; Wu et al., 2009). The DNA-PK holoenzyme is formed when DNA-PKcs binds to Ku at DSB ends and provides DNA end recognition

Correspondence to Patrick Calsou: calsou@ipbs.fr

B. Salles's present address is TOXALIM Research Centre in Food Toxicology, Unité Mixte de Recherche 1331, Institut National de la Recherche Agronomique/Institut National Polytechnique de Toulouse/Université Paul Sabatier, Toulouse F-31027, Cedex 3, France.

Abbreviations used in this paper: ATM, Ataxia telangiectasia mutated; Cali, Calicheamicin γ1; Cer, Cernunnos; DNA-PK, DNA-dependent protein kinase; DNA-PKcs, DNA-PK catalytic subunit; ds, double stranded; DSB, double-strand breaks; IR, ionizing radiation; LIG4, Ligase IV; NHEJ, nonhomologous end joining; V(D)J, variable (diversity) joining; X4, XRCC4; XLF, X4-like factor.

The Rockefeller University Press $30.00
J. Cell Biol. Vol. 200 No. 2 173–186
www.jcb.org/cgi/doi/10.1083/jcb.201203128

and protection activities followed by bridging of the ends, associated with serine/threonine protein kinase activity (Meek et al., 2008). DNA-PK autophosphorylation mediates a conformational change required for activation of end-processing enzymes, such as the Artemis nuclease (Ma et al., 2002; Goodarzi et al., 2006; Dobbs et al., 2010). End ligation requires the concerted action of LIG4 and X4. In vitro, Cer-XLF stimulates ligation by the X4LIG4 complex (Gu et al., 2007b; Lu et al., 2007; Tsai et al., 2007) and promotes readenylation of LIG4 (Riballo et al., 2009).

Although DNA-PKcs–Ku–DNA and X4LIG4 complexes have been clearly defined, the precise temporal and spatial arrangements of higher order complexes during NHEJ await to be established. Although NHEJ components can be independently recruited to damage sites, a large complex may be necessary to optimize the repair process (Ochi et al., 2010). X4 is recruited to laser-induced damage areas, but DNA-PKcs is physically required to stabilize it (Yano and Chen, 2008). A role of DNA-PKcs in stable localization of X4 at the damage sites was also established for chemically induced DSBs (Drouet et al., 2005). Indeed, the resistance of NHEJ factors to biochemical extraction from damaged chromatin suggests that multiple protein–protein interactions can aid stable assembly of the NHEJ machinery (Drouet et al., 2005, 2006; Wu et al., 2007). However, it is unknown whether a supramolecular complex forms in which the Ku–DNA-PKcs and ligase complexes coexist.

In principle, such an NHEJ supramolecular entity would allow the ligation complex to exert an early role well before the final ligation step. Using in vitro and cellular approaches, we unravel here a major contribution of the X4LIG4 complex to the stabilization of end synapsis and associated DNA-PKcs autophosphorylation during NHEJ. Interestingly, the ligase catalytic activity is not required for the synaptic function of the ligation complex. In addition, we show that Cer-XLF also contributes to this noncatalytic function of the ligation complex. Our data support a model in which a supramolecular complex, comprising both Ku–DNA-PKcs and ligase complexes, assembles early during NHEJ and then operates coordinately throughout the repair reaction. By regulating end processing via DNA-PKcs autophosphorylation, this novel noncatalytic activity of the ligase complex may contribute to the maintenance of genomic stability during DSB repair.

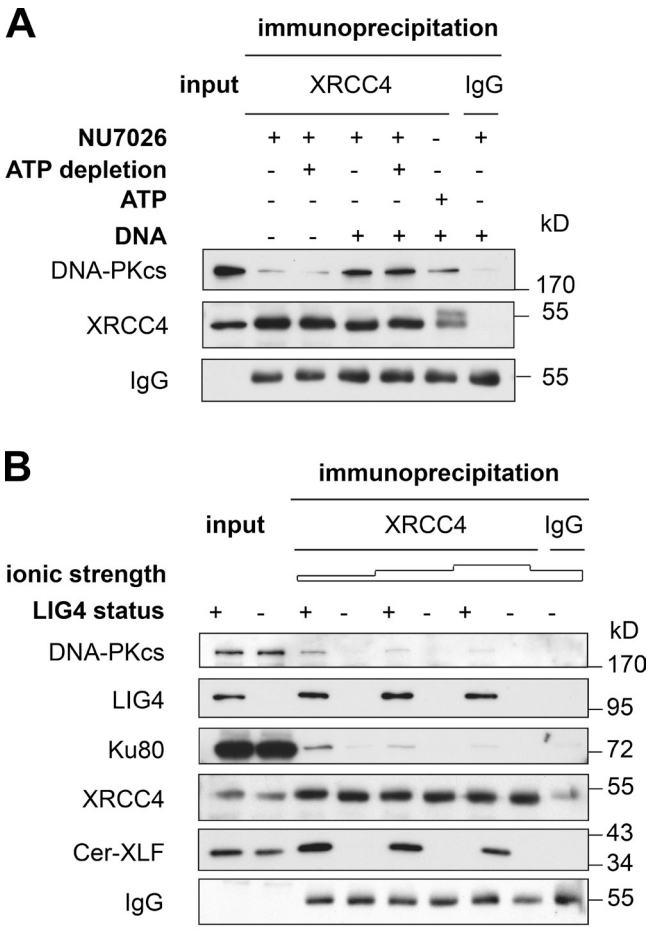

Figure 1. **LIG4 is required for DNA-dependent coimmunoprecipitation of X4, Cer-XLF, and DNA-PK.** (A) Nalm6 extracts were incubated for 15 min under in vitro NHEJ conditions and with components as indicated. ATP depletion refers to addition of the ATP-consuming system (glucose + hexokinase) as previously described (Calsou et al., 2003). Then, the samples were mixed with control IgG or anti-X4 magnetic beads. Immunoprecipitation proceeded for 4 h at 4°C on a wheel followed by three washes for 5 min in 0.5× PBS adjusted to a 100-mM final NaCl concentration, denaturation, and separation on 10% SDS-PAGE gel. The input lane corresponds to 50% of the volume of extracts used in the immunoprecipitation. (B) NHEJ-type extracts from Nalm6 control or N114P2 *LIG4*-null pre-B cells (LIG4 status + or −, respectively) were incubated with ds DNA and NU7026 as defined in A. Incubation was followed by immunoprecipitation with control IgG or anti-X4 antibodies and washes with increasing salt concentration (100, 150, or 200 mM NaCl). Reaction samples were heat denatured, separated on SDS-PAGE gels, and electrotransferred onto membrane that was blotted with antibodies as indicated. The input lanes correspond to 50% of the volume of extracts used in the immunoprecipitation.

Results

LIG4 protein stimulates DNA-PKcs autophosphorylation in vitro

The indispensable step in the NHEJ reaction is the initial assembly of DNA-PK on DNA ends. Addressing the hypothesis that the ligation complex participates in early steps during NHEJ, we reasoned that this would require interaction with DNA-PK. Therefore, we first tested the association of the ligation complex with the DNA-bound DNA-PK in an assay using X4 immunoprecipitation from NHEJ-competent cell extracts incubated with a double-stranded (ds) DNA oligonucleotide (Fig. 1 A). To evaluate the impact of LIG4, we used cell extracts of the N114P2 human pre-B cell line that has targeted disruption in both *LIG4* alleles (Grawunder et al., 1998) and of its wild-type isogenic parental line, Nalm6, as a control. As expected from the high stability of the X4LIG4 complex (Critchlow et al., 1997), LIG4 was present in X4 immunoprecipitates under all salt concentrations during washing (Fig. 1 B). Strikingly, DNA-PKcs and Ku from *LIG4*-null extracts were loosely attached to X4 immunoprecipitates when compared with control extracts, even with the lower salt concentrations during washing (Fig. 1 B). Interestingly, Cer-XLF was recovered on X4 immunoprecipitates from control but not *LIG4*-null extracts (Fig. 1 B). These results are in agreement with data published by our group and others, which have shown that LIG4 is necessary to stabilize the DNA-PK–dependent recruitment of X4 and Cer-XLF to damaged chromatin

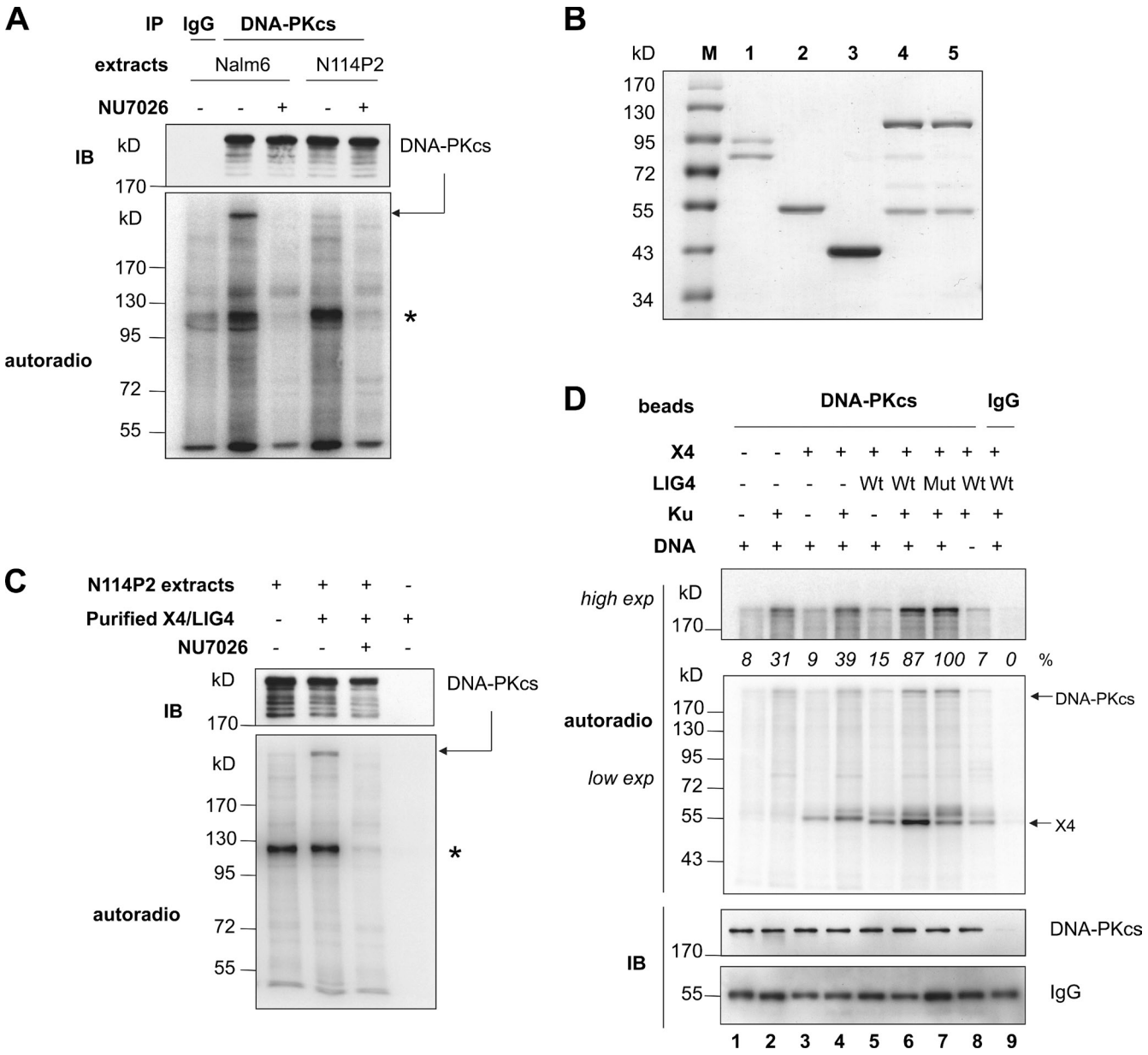

Figure 2. **LIG4 protein, but not activity, is required for DNA-PKcs autophosphorylation activated by ds DNA ends in cell extracts.** (A) Nalm6 control and N114P2 *LIG4*-null extracts were incubated under reaction conditions with γ-[^{32}P]ATP and addition of components as specified. Incubation was followed by immunoprecipitation (IP) with control IgG2a or anti–DNA-PKcs antibodies. Reaction samples were heat denatured, separated on SDS-PAGE gels, and electrotransferred onto membrane that was blotted with antibodies as indicated. (B) Purified proteins Ku70/Ku80 heterodimer (1), X4 (2), Cer-XLF (3), and wild-type (4) or mutant (5) X4LIG4 complexes were loaded on a 10% SDS-PAGE gel and stained with InstantBlue (Euromedex). M, molecular mass markers. (C) Conditions were as in A with N114P2 *LIG4*-null extracts and addition of wild-type X4LIG4 complex as specified followed by DNA-PKcs immunoprecipitation. (D) Purified DNA-PKcs or control IgG on beads were incubated under reaction conditions with γ-[^{32}P]ATP and components as indicated. Wt or Mut refer to wild-type or the catalytically inactive X4LIG4 complex. Low or high exposures of the same membrane are shown. Results of quantitative analysis of the gel are shown as the percentage of the highest phospholabeled DNA-PKcs band after subtraction of background value in the control IgG lane. Autoradio, autoradiography; IB, immunoblotting of the same membrane; exp, exposure. The asterisks indicate a protein coimmunoprecipitated with DNA-PKcs.

(Drouet et al., 2005; Wu et al., 2007; Jayaram et al., 2008). We conclude that LIG4 is necessary for the interaction of the ligation complex with DNA-PK bound to DNA.

Because assembly of DNA-PK on DNA ends leads to DNA-PKcs activation, we next studied the influence of the ligation complex on DNA-PKcs autophosphorylation in vitro, with cell extracts or purified proteins. Thus, Nalm6 and N114P2 *LIG4*-null extracts were incubated with activator DNA and γ-[^{32}P]ATP. After DNA-PKcs immunoprecipitation, samples were fractionated by electrophoresis, and ^{32}P incorporation was assessed by a phosphorimager (see Fig. S1 A for the validation of DNA-PKcs immunoprecipitation). Incubation of Nalm6 extracts promoted phosphorylation of DNA-PKcs and of a coimmunoprecipitated protein that was prevented by NU7026, a specific DNA-PK inhibitor (Fig. 2 A). Under these conditions, *LIG4*-null extracts showed a clear reduction in DNA-PKcs autophosphorylation (mean ratio of 12.1, $n = 5$), whereas DNA-PK–dependent phosphorylation of the coimmunoprecipitated protein

was preserved. Then, we complemented the *LIG4*-null cell extracts with the purified wild-type X4LIG4 complex (see Fig. 2 B for purity control and Fig. S1 B for activity; no DNA-PKcs protein or activity was detected in the purified preparations; Fig. 2 C). DNA-PKcs radiolabeling was strongly stimulated upon addition of wild-type X4LIG4 complex and remained sensitive to NU7026, showing that it relied on DNA-PKcs autophosphorylation (Fig. 2 C).

To directly assess the effect of the ligation complex on DNA-PKcs autophosphorylation, we then performed similar experiments with a simplified protein mixture. DNA-PKcs preparation essentially devoid of the other NHEJ proteins was obtained by immunoprecipitation from Nalm6 cell extracts followed by extensive high-salt wash (Fig. S1, C and D). Importantly, the resulting DNA-PKcs activity was dependent on the addition of purified Ku and DNA and was sensitive to a specific DNA-PKcs inhibitor (Fig. S1 E). Then, purified Ku, X4, or X4LIG4 proteins were added to DNA-PKcs or control IgG beads (see Fig. 2 B for purity control). The Ku- and DNA-dependent autophosphorylation of DNA-PKcs did not vary upon X4 addition (Fig. 2 D, lanes 2 and 4), but the X4LIG4 complex clearly enhanced DNA-PKcs phospholabeling (mean ratio of DNA-PKcs phosphorylation with Ku–X4LIG4 combination over Ku alone = 2.4, $n = 5$; Fig. 2 D, lane 6). In addition, a similar effect was obtained upon addition of an inactive mutant X4LIG4 complex (Fig. 2 D, lane 7; and see Fig. S1 B for absence of ligase activity). Of note, X4 was phosphorylated mainly in a DNA-dependent mode by DNA-PKcs (Fig. 2 D, compare lanes 6 and 8). Together, these data establish that LIG4 associated with X4 is a strong stimulator of DNA-PKcs autophosphorylation in vitro and that the ligase catalytic activity is not required.

Cer-XLF participates in LIG4-dependent DNA-PKcs autophosphorylation in vitro

Because Cer-XLF is a component of the ligation complex, it may participate in the interaction with DNA-PK bound to DNA. Indeed, we made several observations that confirmed this hypothesis. First, the X4 immunoprecipitation assay was performed with extracts from Cer-XLF–deficient BuS cells and Cer-XLF–complemented BuC cells (Buck et al., 2006; Wu et al., 2007). Dissociation of DNA-PKcs and Ku from X4 immunoprecipitates promoted by increasing salt concentrations was enhanced in the absence of Cer-XLF (Fig. 3 A). Second, extracts from Cer-XLF–deficient cells showed a slight decrease in DNA-PKcs autophosphorylation in vitro that was complemented with Cer-XLF purified protein (Fig. S1 F). Of note, purified Cer-XLF did not complement the defect in DNA-PKcs autophosphorylation of *LIG4*-null extracts, indicating that LIG4 was required (Fig. S1 G). Finally, to definitively establish a role for Cer-XLF in DNA-PKcs autophosphorylation in vitro, we activated DNA-PKcs beads with DNA in the presence of purified Ku, X4LIG4, or Cer-XLF purified proteins. As shown in Fig. 3 B, optimal DNA-PKcs phospholabeling was obtained with the combination of all three purified components on DNA-PKcs beads when compared with any combination of two of these components (mean ratio of DNA-PKcs phosphorylation with Ku–X4LIG4–Cer-XLF over Ku–X4LIG4 combination = 1.9, $n = 3$; Fig. 3 B, lane 9). It is noteworthy that Cer-XLF was phosphorylated in the reaction. Altogether, these data indicate that Cer-XLF contributes to LIG4-dependent autophosphorylation of DNA-PKcs in vitro.

LIG4 is a major factor in DNA-PKcs–mediated DNA end synapsis in vitro

In the course of the aforementioned experiments, we noticed that *LIG4*-null cell extracts were not intrinsically defective in DNA-PKcs autophosphorylation. Indeed, increasing the length of the activating ds probe revealed a strong DNA-PKcs autophosphorylation in N114P2 extracts, detected by radiolabeling and comparable to that obtained in the control Nalm6 extracts (Fig. 4 A, compare lanes 3 and 7). In addition, this LIG4-independent DNA-PKcs autophosphorylation mediated by a 250-bp ds probe was strongly repressed by blocking one end with a biotin–streptavidin complex (Fig. 4 A, lane 9). Among other effects, DNA-PKcs autophosphorylation promotes its release from the DNA break (Meek et al., 2008). Indeed, we observed that detachment of DNA-PKcs from the Ku–DNA complex relied on LIG4 with the short probe, whereas this requirement was looser with the long probe (unpublished data).

Elegant approaches in cells and in vitro using combinations of kinase-defective and site-specific nonphosphorylatable mutants of DNA-PKcs have demonstrated that DNA-PKcs autophosphorylation at position S2056 can occur in trans after synapsis mediated by DNA-PK complexes bound to adjacent ends of the DSB (Meek et al., 2007). Thus, the effect of the DNA probe length on DNA-PKcs autophosphorylation was checked by immunoblotting with a phosphospecific antibody that recognizes phosphorylated S2056 (Meek et al., 2007). Phosphorylation of DNA-PKcs at S2056 was clearly detected on the whole-cell extracts (Fig. 4 B, left). A comparison of extracts from Nalm6 and *LIG4*-null cells revealed that LIG4-deficient extracts showed a strong reduction in DNA-PKcs phosphorylation on S2056 with the short DNA probe (Fig. 4 B, right, lanes 7 and 8), in agreement with the results from radiolabeling experiments. However, DNA-PKcs autophosphorylation in *LIG4*-null cells was restored to normal levels with the longer probe but repressed by blocking one end with a biotin–streptavidin complex (Fig. 4 B, right, compare lanes 9 and 10). During the reaction with control extracts, we also observed an X4 phosphorylation as detected by a mobility shift (Fig. 4 B, left), consistent with published findings (Calsou et al., 2003). Notably, *LIG4*-null cell extracts also showed a defect in X4 phosphorylation with the short DNA probe that was restored with the long DNA probe (Fig. 4 B, right).

It has been shown in vitro that DNA end bridging favors global DNA-PK autophosphorylation and that long probes allow intramolecular synapsis, whereas short ds probes only promote intermolecular synapsis (Weterings et al., 2003). Because we found that DNA-PKcs autophosphorylation is defective in *LIG4*-null extracts only when activated with a short DNA probe, this suggests that LIG4 is required for optimal intermolecular synapsis of two DNA ends by DNA-PKcs. The looser LIG4 requirement for DNA-PKcs autophosphorylation with a long activating probe most probably relies on the bending capacity of

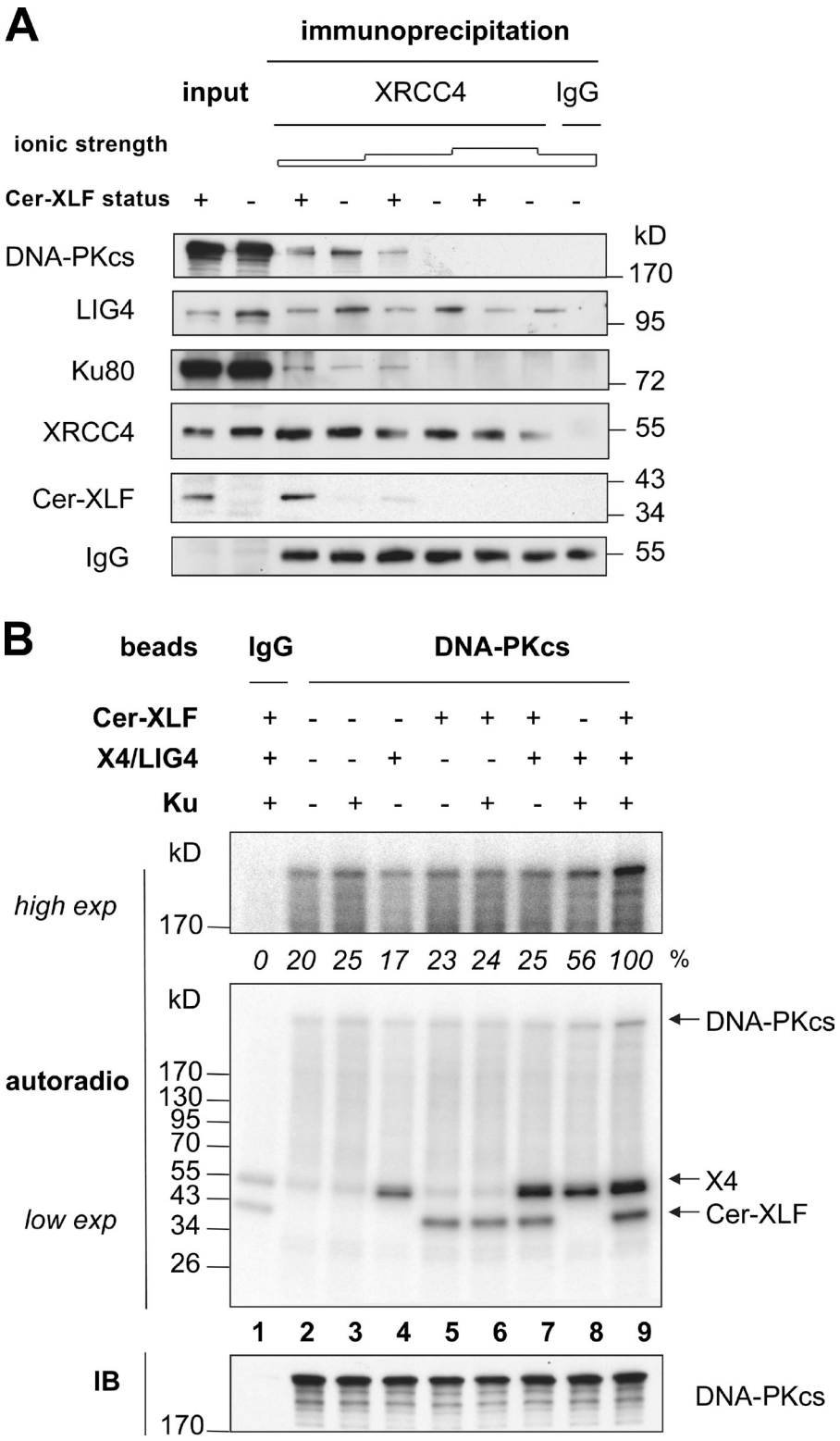

Figure 3. **Effect of Cer-XLF on coimmunoprecipitation of DNA-PK with the ligation complex and on DNA-PKcs autophosphorylation.** (A) NHEJ-type extracts from BuC or BuS fibroblasts (Cer-XLF status + or −, respectively) were incubated with ds DNA and NU7026 as defined in Fig. 1. Incubation was followed by immunoprecipitation with control IgG or anti-X4 antibodies and washes with increasing salt concentration (100, 150, or 200 mM NaCl). Reaction samples were heat denatured, separated on SDS-PAGE gels, and electrotransferred onto membranes that were blotted with antibodies as indicated. (B) Purified DNA-PKcs or control IgG on beads were incubated under reaction conditions with γ-[^{32}P]ATP and purified components as indicated. Low or high exposures of the same membrane are shown. Results of quantitative analysis of the gel are shown as the percentage of the highest phospholabeled DNA-PKcs band after subtraction of background value in the control IgG lane. Autoradio, autoradiography; IB, immunoblotting of the same membrane; exp, exposure.

the probe (Weterings et al., 2003), likely allowing an intramolecular contact of DNA-PK molecules bound at each end, which otherwise can be prevented by streptavidin-mediated hindrance at the biotinylated end.

To directly focus on end synapsis during NHEJ, we then adapted a reported assay (Fig. S2 A; DeFazio et al., 2002). In brief, we synthesized a 502-bp ds DNA fragment that was either biotinylated at one end (502bio) or radiolabeled (502*). NHEJ competent extracts from human cells were incubated with 502* and 502bio bound to streptavidin-coated magnetic beads. The beads were then washed in mild salt buffer, and the radioactivity recovered with the beads was measured by scintillation counting. Control experiments without extracts or 502bio were run in parallel to determine unspecific background (Fig. S2 B).

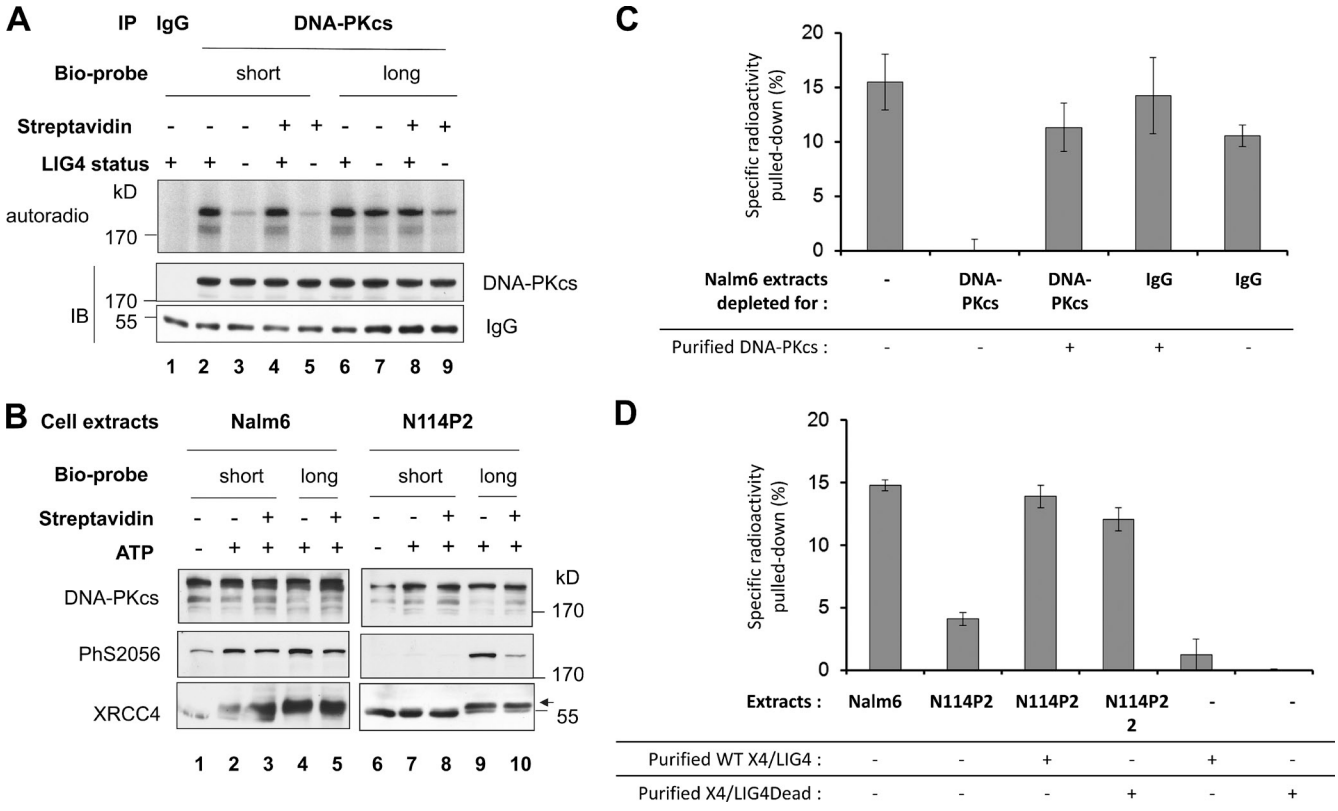

Figure 4. **LIG4 protein, but not activity, stimulated DNA-PK–mediated DNA ends synapsis in vitro.** (A) NHEJ-type extracts from Nalm6 control or N114P2 *LIG4*-null cells (LIG4 status + or −, respectively) were incubated with short (32 bp) or long (250 bp) ds activator DNA under reaction conditions with γ-[^{32}P]ATP and added components as specified. When necessary, the DNA probe was preincubated with streptavidin before addition to the reaction. Incubation was followed by immunoprecipitation with control IgG2a or anti–DNA-PKcs antibodies. Reaction samples were heat denatured, separated on SDS-PAGE gels, and electrotransferred onto membranes that were blotted with antibodies as indicated. Autoradio, autoradiography; IB, immunoblotting of the same membrane; IP, immunoprecipitation. (B) Conditions were as in A but without radiolabeling. The arrow indicates the position of the phosphorylated form of X4. (C and D) Quantification of the specific radioactivity pulled down after subtraction of the unspecific background obtained without the 502bio probe, under conditions of extracts and added components as specified. Each value is the mean of three experiments. Error bars correspond to SEM. WT, wild type.

After background subtraction, we estimated that ∼15% of 502* was specifically pulled down on the streptavidin beads (Fig. 4 C). Titration of an unlabeled DNA fragment inhibited pull-down of the labeled fragment at the expected molar concentration (unpublished data). Because the NHEJ reaction relies on DNA-PKcs activation, extracts were treated with an ATP-consuming system to preclude any ligation from taking place (Calsou et al., 2003). As anticipated, no radioactivity was pulled down in the presence of 500 mM salt and 1% Triton X-100 (Fig. S2 B). In contrast, the radioactivity pulled down was restored upon addition of ATP during the incubation despite the harsh washing conditions (Fig. S2 C), implying that the radiolabeled DNA specifically attached to the beads not only relies on a protein-mediated bridging of the two probes but also on formation of a DNA end synaptic complex prone to ligation.

Various approaches have suggested that DNA-PKcs is responsible for the formation of a synaptic bridge between the two ends of the broken DNA (DeFazio et al., 2002; Weterings et al., 2003; Spagnolo et al., 2006). Thus, extracts were depleted of DNA-PKcs (Fig. S2 D) and assessed for synaptic activity. Synaptic activity was completely lost upon DNA-PKcs depletion and mostly restored upon addition of equivalent amount of the purified protein (Fig. 4 C). Under these conditions, the synapsis activity also relied on Ku (Fig. S2 E). Despite the reported synaptic activity of Ku alone in vitro (Ramsden and Gellert, 1998), this result consolidates the proposal that in a physiological context, DNA-PKcs is essential for synapsis (DeFazio et al., 2002). Moreover, although an intrinsic, transient end bridging activity of the X4LIG4 complex must occur during ligation by this complex (Leber et al., 1998; Chen et al., 2000; Gu et al., 2007a), we have described here a much more stable end bridging (synapsis) by X4LIG4 in the presence of DNA-PKcs.

Finally, the synaptic activity was measured in parallel in extracts from *LIG4*-null N114P2 and parental Nalm6 cells (Fig. 4 D). Strikingly, the synaptic activity was strongly reduced in the absence of LIG4 but restored upon addition of purified X4LIG4 complex to N114P2 extracts, although the purified complex alone did not exhibit a significant synaptic activity (Fig. 4 D). Moreover, although the mutant X4LIG4 complex exhibited no detectable synaptic activity alone, it significantly complemented the synaptic defect of *LIG4*-null extracts (Fig. 4 D).

Defective DSB-induced DNA-PKcs autophosphorylation in cells in the absence of LIG4

Among several phosphorylation sites on DNA-PKcs in cells, phosphorylation on S2056 is believed to be primarily a DSB-induced

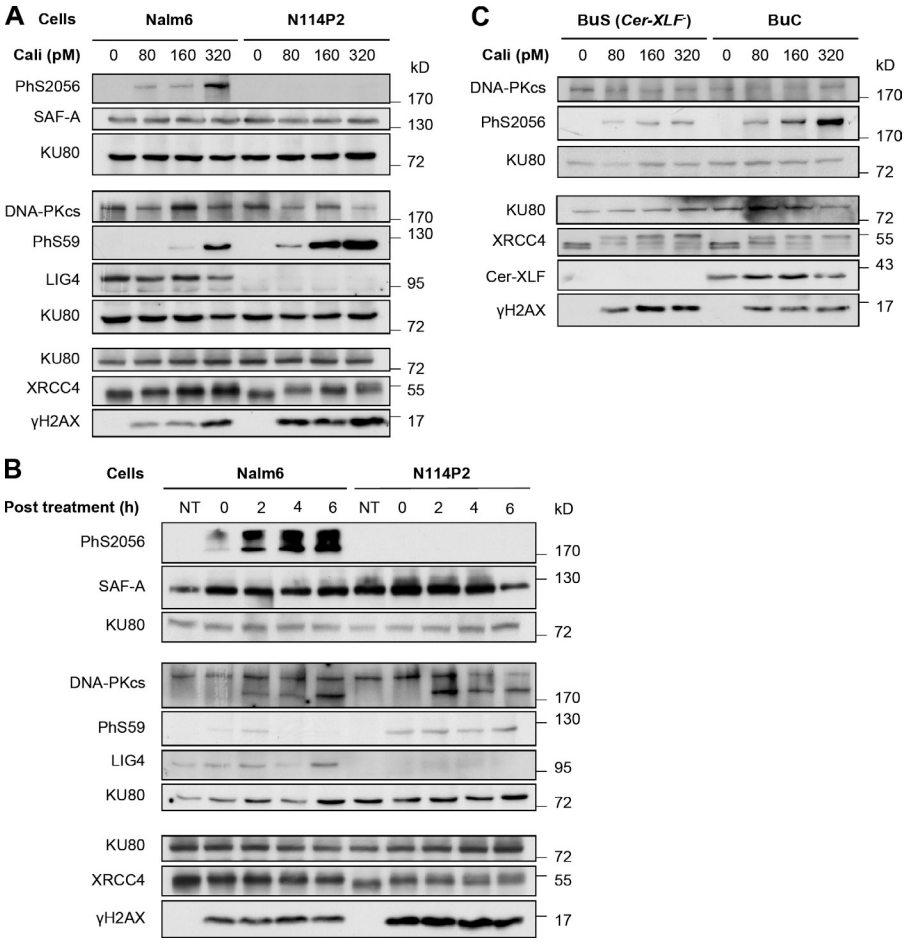

Figure 5. **Requirement of LIG4 for DSB-stimulated DNA-PKcs autophosphorylation in cells and contribution of Cer-XLF.** (A and B) Nalm6 control and N114P2 *LIG4*-null pre-B cells were treated for 1 h with increasing doses of Calicheamicin γ1 (Cali) as indicated (A) or with 160 pM Cali followed by incubation in fresh medium under normal growth conditions for the specified time (B). Whole-cell extracts were heat denatured, separated on SDS-PAGE gels, and electrotransferred onto membranes that were blotted with antibodies as indicated. Protein samples were separated on 8% acrylamide SDS-PAGE gels for standard separation or 15% for γ-H2AX isolation. (C) Western blotting on the whole-cell extracts of BuC control and BuS *Cer-XLF* mutant fibroblasts after treatment with increasing doses of Cali as indicated for 1 h. NT, not treated; PhS59, phosphorylation of SAF-A on S59.

autophosphorylation event (Chen et al., 2005; Cui et al., 2005; Douglas et al., 2007). As a result, phosphorylation on S2056 after DSB production is abolished by a specific DNA-PKcs inhibitor but insensitive to an Ataxia telangiectasia mutated (ATM) kinase inhibitor (Fig. S3 A). Looking for a potential requirement of the ligation complex in early NHEJ steps, we compared DNA-PKcs S2056 autophosphorylation after treatment with Calicheamicin γ1 (Cali) of N114P2 and Nalm6 cells. Cali yields a high ratio of DSBs to single-strand breaks in vivo compared with ionizing radiation (IR; Elmroth et al., 2003). Both cell lines were treated with increasing doses of Cali for 1 h (Fig. 5 A). Strikingly, no phosphorylation of DNA-PKcs on S2056 was detectable in *LIG4*-null cells after Cali treatment, whereas sensitive and dose-dependent S2056 phosphorylation was detected in Nalm6 cells (Fig. 5 A). X4 and SAF-A are DNA-PKcs substrates in cells and can be used to monitor DNA-PKcs activity (Drouet et al., 2005; Britton et al., 2009). In contrast to DNA-PKcs, X4 and SAF-A were phosphorylated at all Cali doses in *LIG4*-null cells. Although S2056 phosphorylation was detectable 6 h after Cali treatment in Nalm6 cells, it remained undetectable in *LIG4*-null cells, despite persistent X4 and SAF-A phosphorylation (Fig. 5 B). The S2056 phosphorylation defect in N114P2 cells compared with their wild-type isogenic counterpart was confirmed in a dose–response experiment using IR (Fig. S3 B) and was observed even after a high IR dose and long time postirradiation (Fig. S3 C).

To extend this observation, exposure to Cali was performed on control AHH1 and LB2304 cells bearing truncating mutations in *LIG4* and in which LIG4 expression is undetectable (Fig. S3, D and E; O'Driscoll et al., 2001). Similar to the data obtained with N114P2 cells, dose–response and time course experiments showed a strong reduction in S2056 DNA-PKcs phosphorylation in LB2304 LIG4-deficient cells, whereas phosphorylation of DNA-PKcs substrates was preserved (Fig. S3, D and E). Because DNA-PK–dependent phosphorylation of nuclear substrates did occur in LIG4-defective cells, the defect in these cells is not a general inhibition of DNA-PK activity but is confined to DNA-PKcs autophosphorylation.

Exploring a role for Cer-XLF, we compared S2056 phosphorylation after treatment with Cali of Cer-XLF–deficient BuS cells and Cer-XLF–complemented BuC cells. Although less pronounced than in LIG4-deficient cells, a partial defect in DNA-PKcs autophosphorylation was observed in BUS cells (Fig. 5 C), confirming together with in vitro data a contribution of Cer-XLF to this LIG4-dependent response to DSBs.

DNA-PKcs autophosphorylation in cells requires LIG4 protein but not ligase activity

Given that neither N114P2 nor LB2304 cells express LIG4 protein, it was not possible to distinguish whether DNA-PKcs autophosphorylation required LIG4 protein or LIG4-dependent ligation. Therefore, we used fibroblasts from a LIG4 syndrome

patient who expresses an inactive form of LIG4 to examine DSB-induced phosphorylation of DNA-PKcs S2056. Patient 411BR has an R278H homozygous mutation and two closely linked N-terminal polymorphic changes resulting in two amino acid substitutions (A3V and T9I), a combination that reduces LIG4 adenylation and ligation activities to ∼1% of the wild-type activity without impacting LIG4 protein levels (O'Driscoll et al., 2001; Girard et al., 2004). Increasing doses of Cali enhanced phosphorylation of DNA-PKcs S2056 as well as X4 to similar extents in 411BR and 1BR cells (Fig. S4 A). Moreover, treatment with increasing doses of IR induced similar S2056 phosphorylation in both cell lines (Fig. S4 B). Identical results were also obtained after treatment with Cali or IR of 495GOS, another LIG4 cell line in which an inactivate LIG4 protein is expressed at normal levels (Fig. S4, C and D; Riballo et al., 2009). Collectively, these findings demonstrate that a ligase catalytic defect in LIG4 has no impact on DNA-PKcs autophosphorylation.

To further address the impact of a LIG4 catalytic defect on DNA-PKcs autophosphorylation, we established derivative populations of the N114P2 cell line, which expressed either the wild-type (N114LIGwt) or a catalytically dead (N114LIGdead) LIG4 protein. Although LIG4 was expressed at reduced levels in N114LIGwt compared with the control Nalm6 cells, its resistance to IR was significantly increased compared with N114P2 cells (Fig. S4, E and F). In contrast, N114LIGdead cells that expressed the same level of LIG4 as N114LIGwt cells remained as sensitive to IR as N114P2 *LIG4*-null cells (Fig. S4, E and F). We, therefore, examined S2056 phosphorylation in response to Cali in N114LIGwt and N114LIGdead cells. Expression of wild-type or catalytically inactive LIG4 in the *Lig4*-null cells restored autophosphorylation of DNA-PKcs (Fig. 6, A and B). Similar results were obtained in dose–response experiments using IR (Fig. S4, G and H). Together, our data demonstrate a major LIG4-dependent role for the NHEJ ligation complex in autophosphorylation of DNA-PKcs after genotoxic DSBs and rule out a prominent impact of the ligase catalytic activity per se.

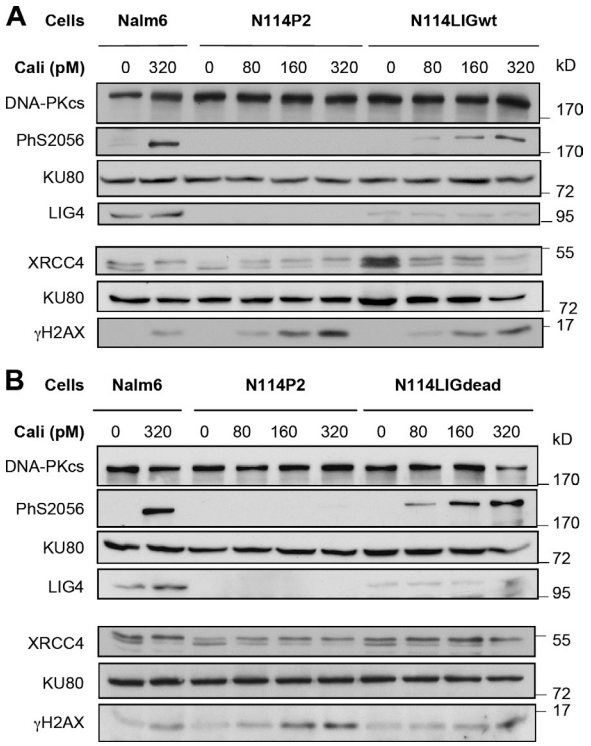

Figure 6. **LIG4 activity is not required for DSB-stimulated DNA-PKcs autophosphorylation in cells.** (A and B) Western blotting on the whole-cell extracts of Nalm6 control cells, N114P2 *LIG4*-null cells, or N114P2 cells expressing wild-type (N114LIGwt) or a catalytic-dead (N114LIGdead) LIG4 protein after treatment for 1 h with increasing doses of Cali as indicated.

Discussion

LIG4 is required for DNA-PKcs autophosphorylation and is a key component in DNA-PK–mediated end synapsis

Our results both in cells and with cell extracts show that X4LIG4 regulates DNA-PKcs autophosphorylation. Of note, Lu et al. (2008) have incidentally observed in reconstituted variable (diversity) joining (V(D)J) recombination reactions that X4LIG4 stimulates DNA-PKcs autophosphorylation mediated by ds DNA oligonucleotides (Lu et al., 2008). In addition, K. Meek and coworkers have also found reduced DNA-PKcs autophosphorylation in X4 defective CHO cells (Meek, K., personal communication). The regulation of DNA-PK autophosphorylation by the ligation complex most likely operates via the stabilization of end synapsis. First, DNA-PKcs autophosphorylation at S2056 can occur in trans at the synapse (Meek et al., 2007). Second, we found a close correlation in vitro between DNA-PKcs autophosphorylation and synapsis: in the absence of LIG4, DNA-PKcs autophosphorylation relying on intermolecular synapsis with short DNA probes was defective, whereas it was restored with long probes, allowing intramolecular synapsis. Third and conversely, X4LIG4 restored both DNA-PKcs autophosphorylation and end synapsis.

The role of LIG4 in synapsis as demonstrated here likely involves its interaction with X4. First, LIG4 is physiologically unstable without X4 (Bryans et al., 1999; Foster et al., 2006), and X4 is at least in sixfold molar excess relative to LIG4 (Mani et al., 2010), making a prominent function of the isolated LIG4 protein per se unlikely. Second, the close correlation that we found in vitro between DNA-PK–dependent phosphorylation of X4, S2056 phosphorylation, and LIG4-dependent synapsis strongly suggests that X4 is necessary for LIG4 loading to the DNA-PK–DNA complex.

X4 or Cer-XLF on their own cannot compensate the synapsis defect in the absence of LIG4. Indeed, we report here a defect in DNA-mediated coimmunoprecipitation of DNA-PK and components of the ligation complex in the absence of LIG4. In addition, purified X4 or Cer-XLF cannot stimulate DNA-PKcs autophosphorylation in the absence of LIG4. Moreover, we and others have shown that a defect in LIG4 expression compromises the stable recruitment of X4 and Cer-XLF to DSB in cells (Drouet et al., 2005; Wu et al., 2007; Jayaram et al., 2008). The interaction reported between Ku and LIG4 (Costantini et al., 2007) may be crucial to stabilize X4LIG4 on the assembled DNA-PK–DNA end complex and direct contact between X4 and DNA-PKcs (Leber et al., 1998; Hsu et al., 2002; Wang et al.,

2004) or Ku (Mari et al., 2006) may be insufficient. Consistent with this, Ku enhances X4LIG4 loading onto DNA ends in vitro (Nick McElhinny et al., 2000) and is required in vivo for recruitment of X4LIG4 to damage sites (Mari et al., 2006). Additionally, the role of X4LIG4 in synapsis may rely on the stabilization of Ku and subsequently DNA-PKcs on the DNA ends. In agreement with this, the yeast Dnl4–Lif1 complex stabilizes Ku at DSBs in vivo (Zhang et al., 2007).

Cer-XLF contributes to the noncatalytic function of the ligation complex

Through stabilizing the association between X4LIG4 and DNA-PK bound to DNA ends, Cer-XLF may be necessary to further consolidate end synapsis. Indeed, we found that Cer-XLF contributes to DNA-PKcs autophosphorylation in vitro and in cells, although its function is less prominent than LIG4. This may rely on the direct interaction between Ku and Cer-XLF (Yano et al., 2011), as shown also for their counterparts in yeast (Chen and Tomkinson, 2011). Our data are in agreement with results in yeast showing that Nej1, the Cer-XLF orthologue, stabilizes the binding of Ku on DNA breaks (Chen and Tomkinson, 2011). In addition, these results may explain the reported contribution of Cer-XLF to processing of the break ends through regulation of the conformation change associated with DNA-PKcs autophosphorylation (Akopiants et al., 2009). In V(D)J recombination, it is believed that coding joints show a more stringent requirement for synapsis than the signal joint to promote efficient end joining (see references in Roy et al., 2012). Interestingly, it has been suggested that the redundancy of ATM and Cer-XLF in joining V(D)J DNA rely on an end-bridging activity (Zha et al., 2011). Moreover, recent data showed that mutations disrupting the Cer-XLF–X4 interaction compromise V(D)J coding rather than signal end joining, in line with this end-bridging hypothesis (Roy et al., 2012). Recently, an end-bridging activity of X4–Cer-XLF complexes has been demonstrated in vitro, which is lost upon LIG4 tandem BRCA1 C-terminal domains binding to X4 (Andres et al., 2012). The LIG4 requirement for DNA-PKcs–mediated end synapsis as shown here does not exclude a potential role of X4–Cer-XLF–dependent DNA bridging at some step during the NHEJ process, for instance before DNA-PKcs recruitment to Ku-bound DNA ends, which may then phosphorylate X4 and modulate the X4–Cer-XLF bridging activity (Roy et al., 2012). Also our data do not rule out the potential contribution to synapsis of proteins outside DNA-PK and the ligation complex.

A productive NHEJ supramolecular complex maintains genomic stability

From the present data, we favor a model in which the optimal functional NHEJ complex comprises both the kinase and the ligase activities early in the process. This is in contrast to a sequential model of the NHEJ reaction because our results directly implicate the ligation complex responsible for a final NHEJ ligation step in the early end synapsis step. The presence of the ligation complex has also been shown to be required for the polymerase and nuclease activities in reconstituted cell-free NHEJ reactions (Lee et al., 2003; Budman et al., 2007). Together, these data illustrate that NHEJ components, although capable of acting independently, also evolved to function in a synergistic manner when in close proximity (Lieber, 2010).

The prosynapsis function of human LIG4 described here may be a conservation of the true synapsis activity of its bacterial ancestor ligD, which also relies on a direct interaction with Ku (Brissett and Doherty, 2009). It may also correspond to a similar activity shown recently with the yeast Dnl4–Lif1 counterpart on Ku (Grob et al., 2012). In addition, the Dnl4–Lif1 complex and Nej1, the yeast orthologue of Cer-XLF, stabilize Ku at DSBs in vivo (Zhang et al., 2007; Chen and Tomkinson, 2011). Thus, this noncatalytic activity of the ligation complex in the NHEJ reaction at early steps after end recognition may fulfill an important function, which is conserved through evolution.

What could be the cellular advantages of such a model for DSB repair by NHEJ? The direct implication of the ligation complex in synaptic stability may help prevent DNA end mobility. X4LIG4, in addition to Ku, suppresses chromosome translocations mediated by alternative NHEJ (Guirouilh-Barbat et al., 2007; Simsek and Jasin, 2010), which may be linked to the contribution of the ligation complex to end synapsis. It would be interesting to assess whether the mobility of DNA ends in the absence of LIG4 is increased as reported in the absence of Ku (Soutoglou et al., 2007).

DNA-PK and Cer-XLF–X4LIG4 bound to DNA ends may also synergistically protect them against undesirable nucleolytic activity, in complement to proteins such as 53BP1, phosphorylated H2AX, or MDC1, which most probably operate at an upstream step of the repair process. In class switch recombination for example, the absence of 53BP1 increases end resection and channels repair to microhomology-mediated alternative end joining (Bothmer et al., 2010). Furthermore, 53BP1 deletion in BRCA1-deficient cells promotes resection and error-free repair by homologous recombination, whereas LIG4 deletion does not (Bunting et al., 2010). Synapsis and possibly end-protecting activity of the NHEJ ligation complex might operate downstream. Indeed, X4LIG4 in addition to Ku is known to suppress DSB repair processes, including homologous recombination and single-strand annealing (Stark et al., 2004; Zhang et al., 2007). Ku and X4LIG4 may protect DNA ends from degradation by directly preventing the proteins responsible for extensive end resection from loading onto the ends (Lee et al., 1998; Smith et al., 2003; Karlsson and Stenerlöw, 2007; Wei and Rong, 2007; Zhang et al., 2007; Cheng et al., 2011; Shao et al., 2012).

Additionally, the dependence of DNA-PKcs–mediated synapsis on the ligation complex as demonstrated here emphasizes a coupling between end processing via DNA-PKcs autophosphorylation and end joining, likely contributing to genomic integrity. The presence of the ligation complex at DNA ends before processing may ensure that end modification would be limited to the minimum required for ligation. DNA end access to processing enzymes likely relies on a change in complex conformation under regulation by DNA-PKcs autophosphorylation (Hammel et al., 2010; Morris et al., 2011). The dependence of this autophosphorylation on X4LIG4 may also prevent extensive end processing until the ligation complex is correctly positioned.

Phosphorylation of positions in the PQR site, including S2056, favors inhibition of end processing and homologous recombination (Cui et al., 2005; Meek et al., 2007; Neal et al., 2011). Thus, linking PQR phosphorylation to the positioning of the end-joining complex as shown here allows end processing and homologous recombination to be restrained at those DSBs that can be repaired by NHEJ.

In conclusion, the X4LIG4–Cer-XLF complex, in addition to ligating DNA ends, contributes to the stabilization of DNA-PK–dependent end synapsis during NHEJ, although the ligase catalytic activity is dispensable for the latter activity. Rather than a sequential assembly of NHEJ components, our data suggest establishment of a supramolecular complex at DSBs in which DNA-PK and ligation complexes coexist. By controlling end processing via DNA-PKcs autophosphorylation, this activity of the ligation complex may contribute to maintenance of genomic stability during DSB repair by NHEJ.

Materials and methods

Cell culture

Cells were grown at 37°C in a humidified atmosphere with 5% CO_2 in culture media (Gibco-Invitrogen) supplemented with 10% fetal calf serum, 2 mM glutamine, 125 U/ml penicillin, and 125 µg/ml streptomycin. The human pre-B cell line Nalm6 and its *LIG4*-defective derivative N114P2 obtained by targeted disruption of both *LIG4* alleles at nucleotide position 1,678, as described previously (Grawunder et al., 1998), were maintained in RPMI 1640 medium. Human telomerase reverse transcriptase immortalized human fibroblasts 1BR (control), 411BR, and 495GOS (both LIG4 deficient and isolated from LIG4 patients as previously described; O'Driscoll et al., 2001; Riballo et al., 2009) were grown in Dulbecco's modified Eagle's medium. AHH1 human lymphoblastoid cells (from a normal individual; gift from G. Lenoir, International Agency for Research on Cancer, Lyon, France) and the human lymphoblastoid cells LB2304 (LIG4 deficient and isolated from a LIG4 patient, compound heterozygote for two truncating mutations, C1738T [R580X] and C2440T [R814X], as previously described; O'Driscoll et al., 2001) were grown in RPMI 1640 with 15% fetal calf serum and 1 mM sodium pyruvate (gift from P. Concannon, University of Virginia, Charlottesville, VA). BuS cells, SV40T-transformed, telomerase-immortalized fibroblasts derived from the Cer-deficient P2 patient (homozygous C622T nonsense mutant [R178X]) and BuC fibroblasts obtained after transduction of BuS with pMND-Cer-myc-IRES-GFP retroviral vector expressing a C-terminal myc-his–tagged Cer protein (gift from J.P. de Villartay and P. Revy, Université Paris Descartes, Paris, France; Buck et al., 2006) were grown in RPMI 1640 medium.

Chemicals

Cali, a generous gift from P.R. Hamann (Wyeth Research, Pearl River, NY), was dissolved at 4 mM in ethanol and stored at −70°C. Staurosporine (Sigma-Aldrich), KU55933, and NU7026 (EMD Millipore) were dissolved in DMSO (10 mM stock solution) and stored at −20°C. Small aliquots of stock solutions chemicals were used once.

Oligonucleotides construct and labeling

Synapse (SYN) oligonucleotide was made by annealing oligonucleotide 5′-GATCCAAAACATGGACTCATATGGCCTATGCATTGAGC-3′ with the oligonucleotide 5′-GGCCGCTCAATGCATAGGCCATATAGTCCATGTTTTG-3′. Control nonbiotinylated and biotinylated 502-bp fragments were amplified by PCR with DNA polymerase (Phusion Hot Start; Finnzymes) from pBluescript II KS (−) with nonbiotinylated or biotinylated reverse primer (5′-GCGTTATCCCCTGATTCTGTGG-3′), respectively, and forward primer (5′-GGGCGAATTGGAGCTCCACC-3′). The 502* fragment was radiolabeled with T4 polynucleotide kinase in the presence of 4,500 Ci/mmol γ-[^{32}P]ATP (ICN Pharmaceuticals), and unincorporated γ-[^{32}P]ATP was removed twice by gel filtration (Sepharose G-50; GE Healthcare). The biotinylated 250-bp fragment was amplified by PCR from pBluescript II KS (−) with biotinylated reverse primer as in this paragraph and forward primer (5′-GGGGTGCCTAATGAGTGAGCTAAC-3′).

Antibodies

Polyclonal rabbit antibody anti-pS2056 obtained against phosphopeptide QSYSYSS(Ph)QDRKPTC as previously described (Chen et al., 2005) was a gift from D.J. Chen (University of Texas, Dallas, TX). Mouse monoclonal antibody against SAF-A PhS59 as previously published (Britton et al., 2009) was manufactured by Biotem by using phosphopeptide EPGNGS(Ph)LDLGGDC as an antigen. Rabbit polyclonal anti-X4 was produced in our laboratory against the full-length recombinant human protein. Polyclonal rabbit antibody anti-XLF was obtained from Bethyl Laboratories, Inc. Mouse monoclonal antibodies were anti-Ku70 (N3H10; Thermo Fisher Scientific) and anti-Ku80 (clone 111; Thermo Fisher Scientific), anti–β-Actin (AC-15; Ambion), anti–PARP-1 (4C10-5; BD), anti–γ-H2AX (JBW301; EMD Millipore), anti-ATM (2C1; Genetex), anti–ATM PhS1981 (EMD Millipore), anti–SAF-A (3G6, Santa Cruz Biotechnology, Inc.), and anti–DNA-PKcs (18.2, 25.4, and 42.27; Abcam). Polyclonal rabbit antibodies were anti-LIG4 (Abcam) and anti–Chk2 PhThr68 (Cell Signaling Technology). Peroxidase-conjugated goat anti—mouse or anti–rabbit secondary antibodies were obtained from Jackson ImmunoResearch Laboratories, Inc.

Western blotting

Concentrated loading buffer was mixed with protein samples to final concentration (50 mM Tris-HCl, pH 6.8, 10% glycerol, 1% SDS, 300 mM 2-mercaptoethanol, and 0.01% bromophenol blue). Protein samples were boiled, separated by SDS-PAGE (generally, 100 µg protein per sample), and blotted onto polyvinylidene difluoride membranes (Immobilon-P; EMD Millipore). After 1-h blocking with 5% dry milk in PBS-T (phosphate buffer saline and 0.1% Tween 20), membranes were incubated for 1 h with primary antibody diluted in PBS-T and 1% bovine serum albumin (fraction V; Sigma-Aldrich), washed three times with PBS-T, and then incubated for 1 h with secondary antibodies in PBS-T. Membranes were washed five times with PBS-T, and immunoblots were visualized by enhanced chemiluminescence (ImmunofaxA; Yelen). When necessary, successive rounds of immunoblotting were performed on the same membranes after stripping (Restore Western Blot Stripping Buffer; Thermo Fisher Scientific). In some experiments, two gels were run in parallel for blotting against a phophosite in a given protein and against this protein (shown as separate groups of clustered rows in the corresponding figures). In some other experiments and providing a short incubation with the first anti-pS2056 antibody, an additional blotting on the same membrane was possible with the antibody against DNA-PKcs. To visualize X4 in immunoprecipitation experiments and to avoid cross-reaction with IgG migrating at the same position, rabbit IgG secondary antibody (TrueBlot; eBioscience) was used according to the instructions of the manufacturer.

Purified proteins

DNA-PKcs was a kind gift of D.J. Chen and was purified from HeLa cells as previously described (Cary et al., 1997). Polyhistidine-tagged wild-type LIG4 or K273A catalytic mutant were coexpressed with untagged wild-type X4 (using coexpression pET28a derivative plasmids pMJ4052 and pMJ4054, respectively) in Rosetta/pLysS cells (EMD Millipore) by growth in selective Luria broth medium at 37°C to OD_{600nm} = 0.5 and induction by addition of 1 mM ITPG and further incubation at 15°C for 16 h. Cells were harvested, lysed in Ni-A buffer (20 mM Tris, pH 8.0, 0.5 M NaCl, 10% glycerol, 10 mM imidazole, and 2 mM β-mercapthoethanol), clarified by high speed centrifugation, and loaded on a column (HisTrap HP; GE Healthcare). The column was washed extensively with Ni-A buffer, and the proteins were eluted with Ni-B buffer (Ni-A + 300 mM imidazole). The preparation was dialyzed against buffer S-A (20 mM Hepes, pH 8.0, 0.05 M KCl, 10% glycerol, 1 mM EDTA, and 2 mM DTT), loaded on a HiTrap SP FF (excess untagged X4 did not bind to the column), and eluted using a linear KCl gradient from 0.05 to 0.35. The X4LIG4 complex preparation was diluted to 0.150 KCl, loaded on a HiTrap Q FF, and eluted using a linear KCl gradient from 0.05 to 0.5 M KCl. The peak fractions containing the complex were dialyzed against 20 mM Hepes, pH 8.0, 0.15 M KCl, 10% glycerol, 1 mM EDTA, and 2 mM DTT, aliquoted, and stored at −80°C. X4 and Cer-XLF were expressed in bacteria and purified by Ni–nitrilotriacetic acid affinity and Sepharose Q chromatography as previously described (Junop et al., 2000; Andres et al., 2007).

For purification of DNA-PKcs on beads, DNA-PKcs was immunoprecipitated from Nalm6 extracts as described in the section Immunodepletion and immunoprecipitation, except that antiphosphatases were omitted. After washing in PBS-T, beads were washed twice for 10 min at 4°C on a wheel in 50 mM Hepes, pH 7.5, 0.05% Tween 20, and 450 mM KCl. After a final wash in PBS-T, beads were diluted in EJ buffer (50 mM triethanolamine, pH 8.0, 0.5 mM magnesium acetate, 1 mM DTT, 0.1 mg/ml BSA, and 60 mM

potassium acetate) supplemented with 25% glycerol and stored at −80°C until use.

End-joining extracts and end-joining assay

NHEJ-competent cell extracts were prepared from exponentially growing cells by three freeze/thaw cycles in lysis buffer (25 mM Tris-HCl, pH 7.5, 333 mM KCl, 1.5 mM EDTA, pH 8.0, and 4 mM DTT) containing protease–phosphatase Halt Inhibitor Cocktail (Thermo Fisher Scientific). After 20-min incubation at 4°C, lysates were centrifuged, and the supernatant was dialyzed against a buffer containing 20 mM Tris-HCl, pH 8.0, 100 mM potassium acetate, 20% glycerol, 0.5 mM EDTA, pH 8.0, and 1 mM DTT. Protein concentration was measured using the Bradford assay (Bio-Rad Laboratories), and end-joining extracts were stored at −80°C. The end-joining assay was performed according to our published protocol (Bombarde et al., 2010) as follows: When necessary, extracts were preincubated with NU7026 (Sigma-Aldrich) as indicated for 10 min at 4°C. Pretreated or mock-treated extracts (40 µg) were incubated for 2 h at 25°C in 10 µl of reaction mixture containing 5 ng EcorRI-linearized pBluescript II KS (−) plasmid in EJ buffer with 1 mM ATP added at last to initiate the reaction. Samples were then treated with 100 µg/ml RNase A for 10 min at 37°C and deproteinized. DNA ligation products were separated in 0.7% agarose gels together with DNA ladder mix (0.5–10 kb; GeneRuler; Thermo Fisher Scientific) in one lane and stained with SYBR green (Invitrogen). Fluorescence was detected and analyzed on a fluorimager (Typhoon; Molecular Dynamics). Quantitative analysis of the gel was performed with the ImageJ software (version 1.4; National Institutes of Health).

Immunodepletion and immunoprecipitation

According to our published protocol (Bombarde et al., 2010), DNA-PKcs immunodepletion was carried out in a 65-µl reaction volume containing 20 µl protein A/G-PLUS agarose wet beads (Santa Cruz Biotechnology, Inc.), 1 mg NHEJ-type extracts in EJ buffer, 10 µg anti–DNA-PKcs antibody (clone 25.4), or control IgG2a. After an overnight incubation at 4°C under constant rotation, the supernatant was recovered by spinning, mixed with 20 µl of new protein A/G-PLUS agarose wet beads, incubated for 1 h at 4°C, and spun down again to remove the beads. Sample aliquots were processed for Western blotting, and the remaining extracts were frozen at −80°C until use.

DNA-PKcs immunoprecipitation was performed for 4 h at 4°C in 60 µl PBS-T and protease–phosphatase Halt Inhibitor Cocktail with 60 µg NHEJ-type Nalm6 extracts on 10-µl wet bead volume (M280 anti–mouse Dynabeads; Invitrogen; prepared with anti–DNA-PKcs antibody [clone 25.4] or control IgG2a according to instructions of the manufacturer). Beads were washed twice in excess volume of the same buffer before heat denaturation in loading sample buffer. X4 immunoprecipitation was performed for 4 h at 4°C in 60 µl PBS-T on 10-µl wet bead volume (M280 anti–rabbit Dynabeads; Invitrogen; prepared with anti-X4 or control preimmune serum according to instructions of the manufacturer).

End synapsis assay

0.5 pmol 502bio ds DNA fragment was immobilized on 10 µl streptavidin paramagnetic beads (Dynabeads M280 streptavidin; Invitrogen) as recommended by the manufacturer. NHEJ-competent cell extracts were first incubated for 10 min at 30°C with 2 mM glucose and 0.2 U hexokinase (EMD Millipore) and purified protein or dilution buffer as indicated. 10 µl of mocked or DNA-treated beads was washed in 0.5× PBS and then incubated under gentle agitation in a final 10-µl reaction volume at 16°C for 30 min in EJ buffer with 0.1 pmol radioactive 502* DNA fragment and 40 µg extracts preincubated as above. Supernatant was removed, and wet beads were washed in excess volume of 0.5× PBS. The wash was then pooled with the supernatant, and the beads were assayed using a scintillation counter. Results are expressed as the percentage of radioactivity pulled down after subtraction of the counts in the sample without 502bio on the beads.

In vitro DNA-PKcs activation in cell extracts or with purified components

When necessary, the extracts were preincubated with 40 µM NU7026 and/or purified 1 pmol X4LIG4 complex as indicated for 15 min at 4°C. 60 µg NHEJ-type cell extracts were incubated at 30°C for 15 min in a final 10-µl reaction volume in EJ buffer supplemented or not supplemented with 2 mM ATP (or 0.2 mM ATP and 0.5 µM γ-[^{32}P]ATP where indicated) and typically in the presence of 0.5 pmol SYN ds oligonucleotide. When indicated, biotinylated DNA was mixed with 2 pmol streptavidin (Sigma-Aldrich) and incubated for 10 min at RT before addition to the reaction mixture. Then, samples from unlabeled reactions were mixed with concentrated loading sample buffer to final concentration, boiled, and separated on 6% SDS-PAGE or 4–15% precast gels (Bio-Rad Laboratories) followed by Western blotting. Radiolabeled reactions were mixed with control or anti–DNA-PKcs magnetic beads. After 3-h immunoprecipitation at 4°C, beads were extensively washed and then processed as in this paragraph for the unlabeled samples. For DNA-PKcs activation with purified components, DNA-PKcs on beads or IgG2a control beads, prepared as detailed in the Purified proteins section, were mixed with purified proteins (1 pmol each of Ku70/80, X4, X4LIG4, or Cer-XLF or equivalent volume of dilution buffer, as indicated) for 15 min at 4°C, and then, reactions proceeded with radiolabeling as described in the previous paragraph.

DNA-damaging treatments and protein extraction

For drug exposure, exponentially growing cells were either mock treated or treated with freshly diluted Cali at the specified concentrations in medium at 37°C in culture dishes (attached cells) or in open tubes (8×10^6 cells per sample) and then harvested at the indicated time points. For cell treatment with IR, irradiation was performed in an irradiator (RX-650; Faxitron X-Ray Corporation) at a dose rate of 0.92 Gy/min. Where indicated, the cells were pretreated with KU55933 or NU7026 for 60 min, and the inhibitors were maintained during the genotoxic treatment. Cells were rinsed with PBS, lysed in for 20 min at 4°C in buffer (50 mM Hepes-KOH, pH 7.5, 450 mM NaCl, 1 mM EDTA, 1% Triton X-100, 1 mM DTT, and protease–phosphatase inhibitors cocktail [Thermo Fisher Scientific]), and then sonicated. Protein concentration was measured by the Bradford assay. NHEJ-competent cell extracts were prepared as previously described (Bombarde et al., 2010).

LIG4-expressing vectors and N114P2 cell complementation

Human LIG4 cDNA was a gift from T. Lindahl (Cancer Research UK London Research Institute, London, England, UK; Wei et al., 1995). Human LIG4 cDNA was subcloned by PCR from a pBluescript-SK vector into a modified pBluescript-KS vector allowing in-frame fusion of a FLAG tag encoding the sequence upstream of LIG4 cDNA. LIG4-K273R ligase-dead mutant was obtained by PCR-mediated site-directed mutagenesis using the following primers: 5′-GTTTCTACATAGAAACCcgtCTAGATGGTGAACGTATG-3′ (sense) and 5′-CATACGTTCACCATCTAGacgGGTTTCTATGTAGAAAC-3′ (lowercase letters correspond to the newly introduced mutated codon). The resulting FLAG-LIG4-WT– and FLAG-LIG4-K273R–encoding cDNAs were then subcloned into the pBabe-Hygro retroviral vector (Addgene plasmid 1765; Bob Weinberg, Whitehead Institute/Massachusetts Institute of Technology, Cambridge, MA) between BamHI and EcoRI restriction sites. All vectors were verified by sequencing (MilleGen).

LIG4-expressing retroviruses were produced by transient cotransfection of GP2-293 packaging cells with pBabe-Hygro-LIG4 and pVSV-G (Takara Bio Inc.) plasmids using Lipofectamine reagent (Invitrogen) according to the manufacturers' recommendations. Cell culture supernatants from days 2 and 3 after transfection were used to infect *LIG4*-null N114P2 target cells. Transduced N114P2 cells were selected under 450 µg/ml hygromycin B.

Survival assays

2.5×10^5 cells per point in 1 ml were irradiated at the indicated doses in 12-well plates in an irradiator (RX-650) at a dose rate of 0.92 Gy/min. After 3 d of growth, aliquots of each sample were counted in a cell coulter (Coulter Z2; Beckman Coulter) calibrated at the mean size of the nontreated sample. Cell survival was calculated at each dose as the ratio of the cell number in the treated sample relative to the cell number in the nontreated sample.

Online supplemental material

Fig. S1 describes the set up and test of DNA-PKcs autophosphorylation in vitro with cell extracts or purified proteins. Fig. S2 shows the analysis of DNA end synapsis in vitro. Fig. S3 describes validation of the anti-PhS2056 antibody and its use in cells extracts. Fig. S4 shows the analysis of DSB-stimulated DNA-PKcs autophosphorylation in ligase-dead cells and the characterization of DNA-PKcs autophosphorylation in N114P2 cells expressing wild-type (N114LIGwt) or catalytic-dead (N114LIGdead) LIG4 protein. Online supplemental material is available at http://www.jcb.org/cgi/content/full/jcb.201203128/DC1.

We are indebted to Tomas Lindahl and Bob Weinberg for providing plasmids, P.R. Hamann for the gift of Cali, and J.P. de Villartay, P. Revy, D.J. Chen, and P. Concannon for providing additional material.

This work was partly supported by grants from La Ligue Nationale Contre le Cancer, Electricité de France (Conseil de Radioprotection), and the Institut National Contre le Cancer (X4–XLF–LIG4 [XXL] screen program). J. Cottarel

was supported by a PhD fellowship from La Ligue Nationale Contre le Cancer. Work in the M. Modesti laboratory is supported by the Association for International Cancer Research and the Association pour la Recherche sur le Cancer. P. Calsou is a scientist from Institut National de la Santé et de la Recherche Médicale, France.

Submitted: 23 March 2012
Accepted: 26 December 2012

References

Akopiants, K., R.Z. Zhou, S. Mohapatra, K. Valerie, S.P. Lees-Miller, K.J. Lee, D.J. Chen, P. Revy, J.P. de Villartay, and L.F. Povirk. 2009. Requirement for XLF/Cernunnos in alignment-based gap filling by DNA polymerases lambda and mu for nonhomologous end joining in human whole-cell extracts. *Nucleic Acids Res.* 37:4055–4062. http://dx.doi.org/10.1093/nar/gkp283

Andres, S.N., M. Modesti, C.J. Tsai, G. Chu, and M.S. Junop. 2007. Crystal structure of human XLF: a twist in nonhomologous DNA end-joining. *Mol. Cell*. 28:1093–1101. http://dx.doi.org/10.1016/j.molcel.2007.10.024

Andres, S.N., A. Vergnes, D. Ristic, C. Wyman, M. Modesti, and M. Junop. 2012. A human XRCC4-XLF complex bridges DNA. *Nucleic Acids Res.* 40:1868–1878. http://dx.doi.org/10.1093/nar/gks022

Bombarde, O., C. Boby, D. Gomez, P. Frit, M.J. Giraud-Panis, E. Gilson, B. Salles, and P. Calsou. 2010. TRF2/RAP1 and DNA-PK mediate a double protection against joining at telomeric ends. *EMBO J.* 29:1573–1584. http://dx.doi.org/10.1038/emboj.2010.49

Bothmer, A., D.F. Robbiani, N. Feldhahn, A. Gazumyan, A. Nussenzweig, and M.C. Nussenzweig. 2010. 53BP1 regulates DNA resection and the choice between classical and alternative end joining during class switch recombination. *J. Exp. Med.* 207:855–865. http://dx.doi.org/10.1084/jem.20100244

Brissett, N.C., and A.J. Doherty. 2009. Repairing DNA double-strand breaks by the prokaryotic non-homologous end-joining pathway. *Biochem. Soc. Trans.* 37:539–545. http://dx.doi.org/10.1042/BST0370539

Britton, S., C. Froment, P. Frit, B. Monsarrat, B. Salles, and P. Calsou. 2009. Cell nonhomologous end joining capacity controls SAF-A phosphorylation by DNA-PK in response to DNA double-strand breaks inducers. *Cell Cycle*. 8:3717–3722. http://dx.doi.org/10.4161/cc.8.22.10025

Bryans, M., M.C. Valenzano, and T.D. Stamato. 1999. Absence of DNA ligase IV protein in XR-1 cells: evidence for stabilization by XRCC4. *Mutat. Res.* 433:53–58. http://dx.doi.org/10.1016/S0921-8777(98)00063-9

Buck, D., L. Malivert, R. de Chasseval, A. Barraud, M.C. Fondanèche, O. Sanal, A. Plebani, J.L. Stéphan, M. Hufnagel, F. le Deist, et al. 2006. Cernunnos, a novel nonhomologous end-joining factor, is mutated in human immunodeficiency with microcephaly. *Cell*. 124:287–299. http://dx.doi.org/10.1016/j.cell.2005.12.030

Budman, J., S.A. Kim, and G. Chu. 2007. Processing of DNA for nonhomologous end-joining is controlled by kinase activity and XRCC4/ligase IV. *J. Biol. Chem.* 282:11950–11959. http://dx.doi.org/10.1074/jbc.M610058200

Bunting, S.F., E. Callén, N. Wong, H.T. Chen, F. Polato, A. Gunn, A. Bothmer, N. Feldhahn, O. Fernandez-Capetillo, L. Cao, et al. 2010. 53BP1 inhibits homologous recombination in Brca1-deficient cells by blocking resection of DNA breaks. *Cell*. 141:243–254. http://dx.doi.org/10.1016/j.cell.2010.03.012

Calsou, P., C. Delteil, P. Frit, J. Drouet, and B. Salles. 2003. Coordinated assembly of Ku and p460 subunits of the DNA-dependent protein kinase on DNA ends is necessary for XRCC4-ligase IV recruitment. *J. Mol. Biol.* 326:93–103. http://dx.doi.org/10.1016/S0022-2836(02)01328-1

Cary, R.B., S.R. Peterson, J. Wang, D.G. Bear, E.M. Bradbury, and D.J. Chen. 1997. DNA looping by Ku and the DNA-dependent protein kinase. *Proc. Natl. Acad. Sci. USA*. 94:4267–4272. http://dx.doi.org/10.1073/pnas.94.9.4267

Chen, B.P., D.W. Chan, J. Kobayashi, S. Burma, A. Asaithamby, K. Morotomi-Yano, E. Botvinick, J. Qin, and D.J. Chen. 2005. Cell cycle dependence of DNA-dependent protein kinase phosphorylation in response to DNA double strand breaks. *J. Biol. Chem.* 280:14709–14715. http://dx.doi.org/10.1074/jbc.M408827200

Chen, L., K. Trujillo, P. Sung, and A.E. Tomkinson. 2000. Interactions of the DNA ligase IV-XRCC4 complex with DNA ends and the DNA-dependent protein kinase. *J. Biol. Chem.* 275:26196–26205. http://dx.doi.org/10.1074/jbc.M000491200

Chen, X., and A.E. Tomkinson. 2011. Yeast Nej1 is a key participant in the initial end binding and final ligation steps of nonhomologous end joining. *J. Biol. Chem.* 286:4931–4940. http://dx.doi.org/10.1074/jbc.M110.195024

Cheng, Q., N. Barboule, P. Frit, D. Gomez, O. Bombarde, B. Couderc, G.S. Ren, B. Salles, and P. Calsou. 2011. Ku counteracts mobilization of PARP1 and MRN in chromatin damaged with DNA double-strand breaks. *Nucleic Acids Res.* 39:9605–9619. http://dx.doi.org/10.1093/nar/gkr656

Costantini, S., L. Woodbine, L. Andreoli, P.A. Jeggo, and A. Vindigni. 2007. Interaction of the Ku heterodimer with the DNA ligase IV/Xrcc4 complex and its regulation by DNA-PK. *DNA Repair (Amst.)*. 6:712–722. http://dx.doi.org/10.1016/j.dnarep.2006.12.007

Critchlow, S.E., R.P. Bowater, and S.P. Jackson. 1997. Mammalian DNA double-strand break repair protein XRCC4 interacts with DNA ligase IV. *Curr. Biol.* 7:588–598. http://dx.doi.org/10.1016/S0960-9822(06)00258-2

Cui, X., Y. Yu, S. Gupta, Y.M. Cho, S.P. Lees-Miller, and K. Meek. 2005. Autophosphorylation of DNA-dependent protein kinase regulates DNA end processing and may also alter double-strand break repair pathway choice. *Mol. Cell. Biol.* 25:10842–10852. http://dx.doi.org/10.1128/MCB.25.24.10842-10852.2005

DeFazio, L.G., R.M. Stansel, J.D. Griffith, and G. Chu. 2002. Synapsis of DNA ends by DNA-dependent protein kinase. *EMBO J.* 21:3192–3200. http://dx.doi.org/10.1093/emboj/cdf299

Dobbs, T.A., J.A. Tainer, and S.P. Lees-Miller. 2010. A structural model for regulation of NHEJ by DNA-PKcs autophosphorylation. *DNA Repair (Amst.)*. 9:1307–1314. http://dx.doi.org/10.1016/j.dnarep.2010.09.019

Douglas, P., X. Cui, W.D. Block, Y. Yu, S. Gupta, Q. Ding, R. Ye, N. Morrice, S.P. Lees-Miller, and K. Meek. 2007. The DNA-dependent protein kinase catalytic subunit is phosphorylated in vivo on threonine 3950, a highly conserved amino acid in the protein kinase domain. *Mol. Cell. Biol.* 27:1581–1591. http://dx.doi.org/10.1128/MCB.01962-06

Downs, J.A., and S.P. Jackson. 2004. A means to a DNA end: the many roles of Ku. *Nat. Rev. Mol. Cell Biol.* 5:367–378. http://dx.doi.org/10.1038/nrm1367

Drouet, J., C. Delteil, J. Lefrançois, P. Concannon, B. Salles, and P. Calsou. 2005. DNA-dependent protein kinase and XRCC4-DNA ligase IV mobilization in the cell in response to DNA double strand breaks. *J. Biol. Chem.* 280:7060–7069. http://dx.doi.org/10.1074/jbc.M410746200

Drouet, J., P. Frit, C. Delteil, J.P. de Villartay, B. Salles, and P. Calsou. 2006. Interplay between Ku, Artemis, and the DNA-dependent protein kinase catalytic subunit at DNA ends. *J. Biol. Chem.* 281:27784–27793. http://dx.doi.org/10.1074/jbc.M603047200

Elmroth, K., J. Nygren, S. Mårtensson, I.H. Ismail, and O. Hammarsten. 2003. Cleavage of cellular DNA by calicheamicin gamma1. *DNA Repair (Amst.)*. 2:363–374. http://dx.doi.org/10.1016/S1568-7864(02)00235-5

Foster, R.E., C. Nnakwe, L. Woo, and K.M. Frank. 2006. Monoubiquitination of the nonhomologous end joining protein XRCC4. *Biochem. Biophys. Res. Commun.* 341:175–183. http://dx.doi.org/10.1016/j.bbrc.2005.12.166

Girard, P.M., B. Kysela, C.J. Härer, A.J. Doherty, and P.A. Jeggo. 2004. Analysis of DNA ligase IV mutations found in LIG4 syndrome patients: the impact of two linked polymorphisms. *Hum. Mol. Genet.* 13:2369–2376. http://dx.doi.org/10.1093/hmg/ddh274

Goodarzi, A.A., Y. Yu, E. Riballo, P. Douglas, S.A. Walker, R. Ye, C. Härer, C. Marchetti, N. Morrice, P.A. Jeggo, and S.P. Lees-Miller. 2006. DNA-PK autophosphorylation facilitates Artemis endonuclease activity. *EMBO J.* 25:3880–3889. http://dx.doi.org/10.1038/sj.emboj.7601255

Grawunder, U., D. Zimmer, S. Fugmann, K. Schwarz, and M.R. Lieber. 1998. DNA ligase IV is essential for V(D)J recombination and DNA double-strand break repair in human precursor lymphocytes. *Mol. Cell.* 2:477–484. http://dx.doi.org/10.1016/S1097-2765(00)80147-1

Grob, P., T.T. Zhang, R. Hannah, H. Yang, M.L. Hefferin, A.E. Tomkinson, and E. Nogales. 2012. Electron microscopy visualization of DNA-protein complexes formed by Ku and DNA ligase IV. *DNA Repair (Amst.)*. 11:74–81. http://dx.doi.org/10.1016/j.dnarep.2011.10.023

Gu, J., H. Lu, B. Tippin, N. Shimazaki, M.F. Goodman, and M.R. Lieber. 2007a. XRCC4:DNA ligase IV can ligate incompatible DNA ends and can ligate across gaps. *EMBO J.* 26:1010–1023. http://dx.doi.org/10.1038/sj.emboj.7601559

Gu, J., H. Lu, A.G. Tsai, K. Schwarz, and M.R. Lieber. 2007b. Single-stranded DNA ligation and XLF-stimulated incompatible DNA end ligation by the XRCC4-DNA ligase IV complex: influence of terminal DNA sequence. *Nucleic Acids Res.* 35:5755–5762. http://dx.doi.org/10.1093/nar/gkm579

Guirouilh-Barbat, J., E. Rass, I. Plo, P. Bertrand, and B.S. Lopez. 2007. Defects in XRCC4 and KU80 differentially affect the joining of distal nonhomologous ends. *Proc. Natl. Acad. Sci. USA*. 104:20902–20907. http://dx.doi.org/10.1073/pnas.0708541104

Hammel, M., Y. Yu, B.L. Mahaney, B. Cai, R. Ye, B.M. Phipps, R.P. Rambo, G.L. Hura, M. Pelikan, S. So, et al. 2010. Ku and DNA-dependent protein kinase dynamic conformations and assembly regulate DNA binding and the initial non-homologous end joining complex. *J. Biol. Chem.* 285:1414–1423. http://dx.doi.org/10.1074/jbc.M109.065615

Hartlerode, A.J., and R. Scully. 2009. Mechanisms of double-strand break repair in somatic mammalian cells. *Biochem. J.* 423:157–168. http://dx.doi.org/10.1042/BJ20090942

Hsu, H.L., S.M. Yannone, and D.J. Chen. 2002. Defining interactions between DNA-PK and ligase IV/XRCC4. *DNA Repair (Amst.)*. 1:225–235. http://dx.doi.org/10.1016/S1568-7864(01)00018-0

Jayaram, S., G. Ketner, N. Adachi, and L.A. Hanakahi. 2008. Loss of DNA ligase IV prevents recognition of DNA by double-strand break repair proteins XRCC4 and XLF. *Nucleic Acids Res.* 36:5773–5786. http://dx.doi.org/10.1093/nar/gkn552

Junop, M.S., M. Modesti, A. Guarné, R. Ghirlando, M. Gellert, and W. Yang. 2000. Crystal structure of the Xrcc4 DNA repair protein and implications for end joining. *EMBO J.* 19:5962–5970. http://dx.doi.org/10.1093/emboj/19.22.5962

Karlsson, K.H., and B. Stenerlöw. 2007. Extensive ssDNA end formation at DNA double-strand breaks in non-homologous end-joining deficient cells during the S phase. *BMC Mol. Biol.* 8:97. http://dx.doi.org/10.1186/1471-2199-8-97

Leber, R., T.W. Wise, R. Mizuta, and K. Meek. 1998. The XRCC4 gene product is a target for and interacts with the DNA-dependent protein kinase. *J. Biol. Chem.* 273:1794–1801. http://dx.doi.org/10.1074/jbc.273.3.1794

Lee, J.W., S.M. Yannone, D.J. Chen, and L.F. Povirk. 2003. Requirement for XRCC4 and DNA ligase IV in alignment-based gap filling for nonhomologous DNA end joining in vitro. *Cancer Res.* 63:22–24.

Lee, S.E., J.K. Moore, A. Holmes, K. Umezu, R.D. Kolodner, and J.E. Haber. 1998. *Saccharomyces* Ku70, mre11/rad50 and RPA proteins regulate adaptation to G2/M arrest after DNA damage. *Cell*. 94:399–409. http://dx.doi.org/10.1016/S0092-8674(00)81482-8

Lieber, M.R. 2010. The mechanism of double-strand DNA break repair by the nonhomologous DNA end-joining pathway. *Annu. Rev. Biochem.* 79:181–211. http://dx.doi.org/10.1146/annurev.biochem.052308.093131

Lu, H., U. Pannicke, K. Schwarz, and M.R. Lieber. 2007. Length-dependent binding of human XLF to DNA and stimulation of XRCC4.DNA ligase IV activity. *J. Biol. Chem.* 282:11155–11162. http://dx.doi.org/10.1074/jbc.M609904200

Lu, H., N. Shimazaki, P. Raval, J. Gu, G. Watanabe, K. Schwarz, P.C. Swanson, and M.R. Lieber. 2008. A biochemically defined system for coding joint formation in V(D)J recombination. *Mol. Cell*. 31:485–497. http://dx.doi.org/10.1016/j.molcel.2008.05.029

Ma, Y., U. Pannicke, K. Schwarz, and M.R. Lieber. 2002. Hairpin opening and overhang processing by an Artemis/DNA-dependent protein kinase complex in nonhomologous end joining and V(D)J recombination. *Cell*. 108:781–794. http://dx.doi.org/10.1016/S0092-8674(02)00671-2

Mani, R.S., Y. Yu, S. Fang, M. Lu, M. Fanta, A.E. Zolner, N. Tahbaz, D.A. Ramsden, D.W. Litchfield, S.P. Lees-Miller, and M. Weinfeld. 2010. Dual modes of interaction between XRCC4 and polynucleotide kinase/phosphatase: implications for nonhomologous end joining. *J. Biol. Chem.* 285:37619–37629. http://dx.doi.org/10.1074/jbc.M109.058719

Mari, P.O., B.I. Florea, S.P. Persengiev, N.S. Verkaik, H.T. Brüggenwirth, M. Modesti, G. Giglia-Mari, K. Bezstarosti, J.A. Demmers, T.M. Luider, et al. 2006. Dynamic assembly of end-joining complexes requires interaction between Ku70/80 and XRCC4. *Proc. Natl. Acad. Sci. USA*. 103:18597–18602. http://dx.doi.org/10.1073/pnas.0609061103

Meek, K., P. Douglas, X. Cui, Q. Ding, and S.P. Lees-Miller. 2007. trans Autophosphorylation at DNA-dependent protein kinase's two major autophosphorylation site clusters facilitates end processing but not end joining. *Mol. Cell. Biol.* 27:3881–3890. http://dx.doi.org/10.1128/MCB.02366-06

Meek, K., V. Dang, and S.P. Lees-Miller. 2008. DNA-PK: the means to justify the ends? *Adv. Immunol*. 99:33–58. http://dx.doi.org/10.1016/S0065-2776(08)00602-0

Morris, E.P., A. Rivera-Calzada, P.C. da Fonseca, O. Llorca, L.H. Pearl, and L. Spagnolo. 2011. Evidence for a remodelling of DNA-PK upon autophosphorylation from electron microscopy studies. *Nucleic Acids Res.* 39:5757–5767. http://dx.doi.org/10.1093/nar/gkr146

Neal, J.A., V. Dang, P. Douglas, M.S. Wold, S.P. Lees-Miller, and K. Meek. 2011. Inhibition of homologous recombination by DNA-dependent protein kinase requires kinase activity, is titratable, and is modulated by autophosphorylation. *Mol. Cell. Biol.* 31:1719–1733. http://dx.doi.org/10.1128/MCB.01298-10

Nick McElhinny, S.A., C.M. Snowden, J. McCarville, and D.A. Ramsden. 2000. Ku recruits the XRCC4-ligase IV complex to DNA ends. *Mol. Cell. Biol.* 20:2996–3003. http://dx.doi.org/10.1128/MCB.20.9.2996-3003.2000

Ochi, T., B.L. Sibanda, Q. Wu, D.Y. Chirgadze, V.M. Bolanos-Garcia, and T.L. Blundell. 2010. Structural biology of DNA repair: spatial organisation of the multicomponent complexes of nonhomologous end joining. *J. Nucleic Acids*. 2010:621695.

O'Driscoll, M., and P.A. Jeggo. 2006. The role of double-strand break repair - insights from human genetics. *Nat. Rev. Genet.* 7:45–54. http://dx.doi.org/10.1038/nrg1746

O'Driscoll, M., K.M. Cerosaletti, P.M. Girard, Y. Dai, M. Stumm, B. Kysela, B. Hirsch, A. Gennery, S.E. Palmer, J. Seidel, et al. 2001. DNA ligase IV mutations identified in patients exhibiting developmental delay and immunodeficiency. *Mol. Cell*. 8:1175–1185. http://dx.doi.org/10.1016/S1097-2765(01)00408-7

Pardo, B., B. Gómez-González, and A. Aguilera. 2009. DNA repair in mammalian cells: DNA double-strand break repair: how to fix a broken relationship. *Cell. Mol. Life Sci.* 66:1039–1056. http://dx.doi.org/10.1007/s00018-009-8740-3

Polo, S.E., and S.P. Jackson. 2011. Dynamics of DNA damage response proteins at DNA breaks: a focus on protein modifications. *Genes Dev.* 25:409–433. http://dx.doi.org/10.1101/gad.2021311

Ramsden, D.A., and M. Gellert. 1998. Ku protein stimulates DNA end joining by mammalian DNA ligases: a direct role for Ku in repair of DNA double-strand breaks. *EMBO J.* 17:609–614. http://dx.doi.org/10.1093/emboj/17.2.609

Riballo, E., L. Woodbine, T. Stiff, S.A. Walker, A.A. Goodarzi, and P.A. Jeggo. 2009. XLF-Cernunnos promotes DNA ligase IV-XRCC4 re-adenylation following ligation. *Nucleic Acids Res.* 37:482–492. http://dx.doi.org/10.1093/nar/gkn957

Roy, S., S.N. Andres, A. Vergnes, J.A. Neal, Y. Xu, Y. Yu, S.P. Lees-Miller, M. Junop, M. Modesti, and K. Meek. 2012. XRCC4's interaction with XLF is required for coding (but not signal) end joining. *Nucleic Acids Res.* 40:1684–1694. http://dx.doi.org/10.1093/nar/gkr1315

Shao, Z., A.J. Davis, K.R. Fattah, S. So, J. Sun, K.J. Lee, L. Harrison, J. Yang, and D.J. Chen. 2012. Persistently bound Ku at DNA ends attenuates DNA end resection and homologous recombination. *DNA Repair (Amst.)*. 11:310–316. http://dx.doi.org/10.1016/j.dnarep.2011.12.007

Simsek, D., and M. Jasin. 2010. Alternative end-joining is suppressed by the canonical NHEJ component Xrcc4-ligase IV during chromosomal translocation formation. *Nat. Struct. Mol. Biol.* 17:410–416. http://dx.doi.org/10.1038/nsmb.1773

Smith, J., E. Riballo, B. Kysela, C. Baldeyron, K. Manolis, C. Masson, M.R. Lieber, D. Papadopoulo, and P. Jeggo. 2003. Impact of DNA ligase IV on the fidelity of end joining in human cells. *Nucleic Acids Res.* 31:2157–2167. http://dx.doi.org/10.1093/nar/gkg317

Soutoglou, E., J.F. Dorn, K. Sengupta, M. Jasin, A. Nussenzweig, T. Ried, G. Danuser, and T. Misteli. 2007. Positional stability of single double-strand breaks in mammalian cells. *Nat. Cell Biol.* 9:675–682. http://dx.doi.org/10.1038/ncb1591

Spagnolo, L., A. Rivera-Calzada, L.H. Pearl, and O. Llorca. 2006. Three-dimensional structure of the human DNA-PKcs/Ku70/Ku80 complex assembled on DNA and its implications for DNA DSB repair. *Mol. Cell*. 22:511–519. http://dx.doi.org/10.1016/j.molcel.2006.04.013

Stark, J.M., A.J. Pierce, J. Oh, A. Pastink, and M. Jasin. 2004. Genetic steps of mammalian homologous repair with distinct mutagenic consequences. *Mol. Cell. Biol.* 24:9305–9316. http://dx.doi.org/10.1128/MCB.24.21.9305-9316.2004

Tsai, C.J., S.A. Kim, and G. Chu. 2007. Cernunnos/XLF promotes the ligation of mismatched and noncohesive DNA ends. *Proc. Natl. Acad. Sci. USA*. 104:7851–7856. http://dx.doi.org/10.1073/pnas.0702620104

Wang, Y.G., C. Nnakwe, W.S. Lane, M. Modesti, and K.M. Frank. 2004. Phosphorylation and regulation of DNA ligase IV stability by DNA-dependent protein kinase. *J. Biol. Chem.* 279:37282–37290. http://dx.doi.org/10.1074/jbc.M401217200

Wei, D.S., and Y.S. Rong. 2007. A genetic screen for DNA double-strand break repair mutations in *Drosophila*. *Genetics*. 177:63–77. http://dx.doi.org/10.1534/genetics.107.077693

Wei, Y.F., P. Robins, K. Carter, K. Caldecott, D.J. Pappin, G.L. Yu, R.P. Wang, B.K. Shell, R.A. Nash, P. Schär, et al. 1995. Molecular cloning and expression of human cDNAs encoding a novel DNA ligase IV and DNA ligase III, an enzyme active in DNA repair and recombination. *Mol. Cell. Biol.* 15:3206–3216.

Weterings, E., and D.J. Chen. 2008. The endless tale of non-homologous end-joining. *Cell Res.* 18:114–124. http://dx.doi.org/10.1038/cr.2008.3

Weterings, E., N.S. Verkaik, H.T. Brüggenwirth, J.H. Hoeijmakers, and D.C. van Gent. 2003. The role of DNA dependent protein kinase in synapsis of DNA ends. *Nucleic Acids Res.* 31:7238–7246. http://dx.doi.org/10.1093/nar/gkg889

Wu, P.Y., P. Frit, L. Malivert, P. Revy, D. Biard, B. Salles, and P. Calsou. 2007. Interplay between Cernunnos-XLF and nonhomologous end-joining proteins at DNA ends in the cell. *J. Biol. Chem.* 282:31937–31943. http://dx.doi.org/10.1074/jbc.M704554200

Wu, P.Y., P. Frit, S. Meesala, S. Dauvillier, M. Modesti, S.N. Andres, Y. Huang, J. Sekiguchi, P. Calsou, B. Salles, and M.S. Junop. 2009. Structural and functional interaction between the human DNA repair proteins DNA ligase IV and XRCC4. *Mol. Cell. Biol.* 29:3163–3172. http://dx.doi.org/10.1128/MCB.01895-08

Wyman, C., and R. Kanaar. 2006. DNA double-strand break repair: all's well that ends well. *Annu. Rev. Genet.* 40:363–383. http://dx.doi.org/10.1146/annurev.genet.40.110405.090451

Yano, K.I., and D.J. Chen. 2008. Live cell imaging of XLF and XRCC4 reveals a novel view of protein assembly in the non-homologous end-joining pathway. *Cell Cycle*. 7:1321–1325. http://dx.doi.org/10.4161/cc.7.10.5898

Yano, K.I., K. Morotomi-Yano, K.J. Lee, and D.J. Chen. 2011. Functional significance of the interaction with Ku in DNA double-strand break recognition of XLF. *FEBS Lett.* 585:841–846. http://dx.doi.org/10.1016/j.febslet.2011.02.020

Zha, S., C. Guo, C. Boboila, V. Oksenych, H.L. Cheng, Y. Zhang, D.R. Wesemann, G. Yuen, H. Patel, P.H. Goff, et al. 2011. ATM damage response and XLF repair factor are functionally redundant in joining DNA breaks. *Nature*. 469:250–254. http://dx.doi.org/10.1038/nature09604

Zhang, Y., M.L. Hefferin, L. Chen, E.Y. Shim, H.M. Tseng, Y. Kwon, P. Sung, S.E. Lee, and A.E. Tomkinson. 2007. Role of Dnl4-Lif1 in nonhomologous end-joining repair complex assembly and suppression of homologous recombination. *Nat. Struct. Mol. Biol.* 14:639–646. http://dx.doi.org/10.1038/nsmb1261